Research Article | Vol. 10, No. 10 / 1 October 2019 / Biomedical Optics Express 5351
Biomedical Optics EXPRESS

Study of the dielectric characteristics of living glial-like cells using terahertz ATR spectroscopy

YUYE WANG,[1,2,3] ZHINAN JIANG,[1,2] DEGANG XU,[1,2,5] TUNAN CHEN,[3,6] BEIKE CHEN,[4] SHI WANG,[3] NING MU,[3] HUA FENG,[3] AND JIANQUAN YAO[1,2]

[1]*Institute of Laser and Optoelectronics, School of Precision Instruments and Optoelectronics Engineering, Tianjin University, Tianjin 300072, China*
[2]*Key Laboratory of Optoelectronics Information Technology (Ministry of Education), Tianjin University, Tianjin 300072, China*
[3]*Department of Neurosurgery and Key Laboratory of Neurotrauma, Southwest Hospital, Third Military Medical University (Army Medical University), Chongqing 400038, China*
[4]*The First Affiliated Hospital of Chongqing Medical University, Chongqing 400016, China*
[5]*xudegang@tju.edu.cn*
[6]*ctn_666@sina.com*

Abstract: The attenuated total reflection spectroscopy system with the Si container attached on the prism has been demonstrated as an efficient technique to obtain the dielectric properties of living cells in the THz range. We proposed a method to determine the dielectric responses of living cells based on the combination of the single-interface and two-interface ATR models without cell thickness. The experimental results for living glial-like cells (PC12, SVG P12 and HMO6) showed the dielectric responses in the THz region were related significantly to cell number, intracellular fluid, and cell structure. Moreover, the glioma cells (C6 and U87) exhibited different dielectric properties compared with the glial-like cells, which could be one reason for the glioma tissue diagnosis using THz wave.

1. Introduction

The dielectric properties of living cells are important parameters reflecting cell characteristics. With the fast development of terahertz (THz) technology, the dielectric properties of living cells in the THz region has attracted much attentions for important applications in cancer detection and molecular biology [1–9]. The nervous system is built from two broad categories of cells, neurons and glial cells. For living neurons, it has been proved that the THz wave could induce the changes of membranes potential (MP) [10] and the growth of neurites of sensory ganglia [11]. Additionally, the direct visualization of neuron swelling induced by temperature change was measured by ionic contrast THz (ICT) imaging [12]. Glial cells are widely distributed in the central and peripheral nervous system as supporting cells. They are integral functional elements of the synapses, responding to neuronal activity and regulating synaptic transmission and plasticity [13,14]. It has been confirmed that THz exposure with a certain intensity and duration time can cause cell apoptosis [15], and has impact not only on glial cells but also on other biological systems, such as bacteria and yeast [16]. However, the dielectric responses of the living glial-like cells in the THz region has yet to be explored.

Terahertz time domain spectroscopy system (THz-TDS) has been widely used to detect the spectral properties of different samples, like the refractive index and extinction coefficient. Generally speaking, the transmission mode is preferred for cellular spectroscopy and imaging due to its simplicity. Considering the strong absorption of THz wave by polar liquids, the culture medium in which living cells survive was always removed completely from cell monolayer [17]. Thus, the obtained dielectric responses in the THz region were for dehydrated cells, which

#368682 https://doi.org/10.1364/BOE.10.005351
Journal © 2019 Received 10 Jun 2019; revised 2 Sep 2019; accepted 3 Sep 2019; published 23 Sep 2019

Biomedical Optics EXPRESS

cannot reflect the real characteristics of living cells. Attenuated total internal reflection (ATR) mode has been proven more sensitive for measuring highly absorptive media compared with transmission mode. It is an ideal tool to maintain the viability for cell monolayer. Considering that the penetration depth of THz wave is greater than the thickness of cell monolayer, the ATR spectroscopy combined with a two-interface model was applied in order to determine the dielectric properties of living cells accurately [18]. In this scheme, the living cells were cultured in a fluid culture medium on the surface of the ATR prism, where the cell monolayer was used as layer sample and the liquid culture medium above the cell monolayer was used as bulk sample. Based on two-interface model, the dielectric responses of cultured human cancer cells (DLD-1, HEK293 and HeLa) [19], the permeabilization of living cells [20], the ratio of hydrating water molecules in the living cells [21] and the dynamics of cell death [22] were detected. However, there are still some problems with the above method. Firstly, due to biological diversity, the experiment should be performed repeatedly many times. For each prism allowing only a kind of cells to grow once, the experimental process is time-consuming obviously and the adjustment errors will occur during the replacement of the prism. Secondly, in order to obtain the dielectric properties of living cell monolayer, the thickness of living cell monolayer must be known for the calculation. However, the thickness of living cell monolayer is always hard to be observed accurately, which is on the order of micrometers. The slight error introduced by the cell thickness would have a significant effect on the results of dielectric properties. Thus, there is a high demand for the measurement of cell thickness.

In this paper, we designed reusable Si containers in the same specification to culture the living cells on the bottom of the Si containers. The accuracy of the ATR spectroscopy system with the Si containers attached onto the ATR prism closely was analyzed. The calculation method to determine the dielectric responses of living cells was proposed based on the combination of the single-interface and two-interface sample models. In experiment, the dielectric parameters of the living glial-like cell monolayer were characterized accurately. The influence of cell number and cell type on dielectric responses was investigated by THz-TDS system. Moreover, the glioma cells showed different properties compared with the glial-like cells in the THz region. This method will provide a perspective to characterize the living cells in details.

2. Experimental methods

2.1. Experimental setup

The THz time-domain ATR spectroscopy system (Advantest TAS7500) equipped with a high-resistance Si prism was employed in this research, as shown in Fig. 1(a). The incident angle (57 degree) provided the total internal reflection condition. To realize more measurements on single prism and avoid the errors caused by the replacement of the Si prism, the Si containers was designed as shown in Fig. 1(b), the material of which is same to the Si prism. The shape of the containers was cylindrical, the bottom as well as the top was made of 0.5mm-thickness and 20mm-diameter polished Si wafer, and the side was made of aluminum. The living cells were cultured in the Si containers instead of on the ATR prism. Meantime, the same size container made of quartz was used to observe the cell status. Multiple measurements can be realized by replacing with other Si containers in the same specification. Especially, the empty Si container attached closely onto the ATR prism of the TDS spectrometer was used as the reference. In fact, there was an air layer between the bottom of the Si container and the ATR prism, and the thickness of the air-layer was determined by the pressure above the Si container and the surface cleanliness of ATR prism and Si wafer.

Biomedical Optics EXPRESS

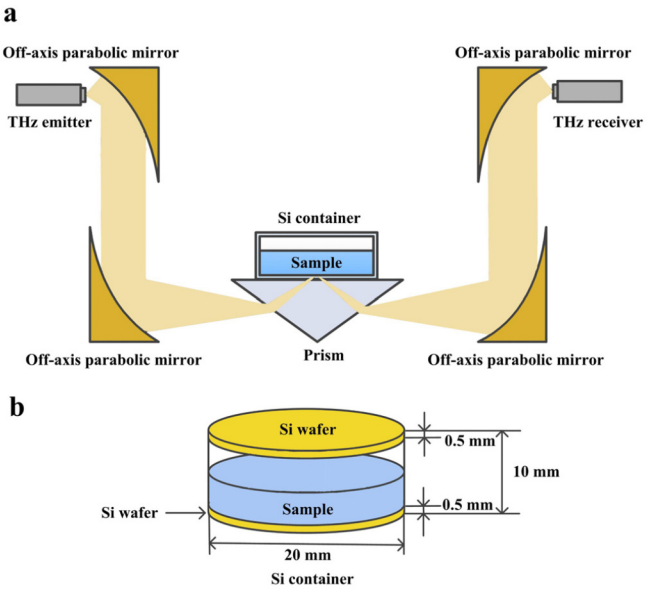

Fig. 1. The schematic illustration of the THz ATR spectroscopy system.

2.2. Sample preparation

The PC12, C6, SVG P12 and HMO6, U87 cells were chosen for the experimental measurement. Neuron, glial cell, and glioma cell are three typical cells in the nervous system. The PC12 cell is a widely used nerve cell line, which can reflect the characteristic of neuron in rat. The SVG P12 human astrocyte and the HMO6 human microglial are important components of the human glial cell. The C6 rat glioma cell and the U87 human glioma cell were chosen to reveal the differences between glioma cell and normal cell. All cell lines were obtained from BeNa Culture Collection (BNCC, Germany). The PC12 cells were cultured in Roswell Park Memorial Institute 1640 medium (RPMI 1640, Gibco, Carlsbad, CA, USA) containing 10% fetal bovine serum (Gibco, Carlsbad, CA, USA), while the C6, SVG P12 and HMO6 cells were cultured in Dulbecco's modified Eagle's medium (DMEM, Gibco, Carlsbad, CA, USA) containing 10% fetal bovine serum (Gibco, Carlsbad, CA, USA), 100 U/mL penicillin and 100 U/mL streptomycin (HyClone Laboratories, Utah, UT, USA). The U87 cells were cultured in DMEM/F12 medium (Gibco, Carlsbad, CA, USA). All cells were cultured in an incubator (Thermo Electron Corporation, USA) at a concentration of 5% carbon dioxide at 37°C. The culture medium was replaced every 3d until the cells reached 90% confluence. The cells were passaged by 0.25% trypsin (HyClone Laboratories, Utah, UT, USA) for 2 mins at room temperature, seeded into the transparent quartz containers and Si containers after calculating the amount of cells needed, and allowed to adhere overnight. Here, the number of cells in the experiment was defined as the total quantity of cells on the surface of a 20mm-diameter silicon wafer. On the following day, the culture medium was replaced before the observation. The homogeneity, growth state and adhesion of cell monolayer in the transparent quartz container was observed under the microscope. Figure 2 showed an example of PC 12 cells with different cell numbers of 2.0×10^5, 3.0×10^5 and 4.0×10^5. We chose cell monolayer with better growth state and homogeneity for THz measurement. To confirm the level of cell confluency in the Si container, the cells were counted from the quartz container and the Si container at the same time using cell counting chamber. For PC12 cells, the results of cell counting in the quartz container and the Si container were $1.9\times10^5/1.85\times10^5$, $3.0\times10^5/2.95\times10^5$ and $3.8\times10^5/3.95\times10^5$, while the original number of cells were 2.0×10^5, 3.0×10^5 and 4.0×10^5,

Biomedical Optics EXPRESS

respectively. The almost same numbers of cell in the two groups indicate the cells can be well adhesive in the Si container.

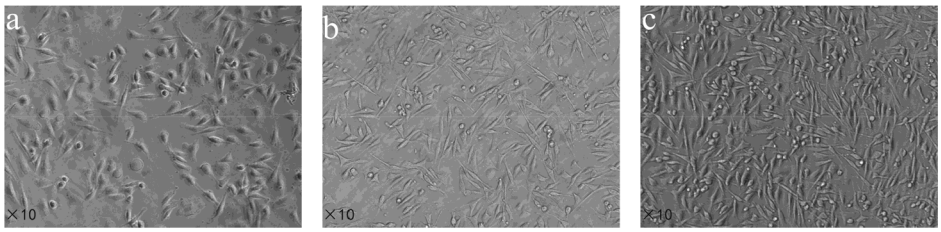

Fig. 2. Microscopy photograph of PC12 cell monolayer with different number. (a) 2.0×10^5 (b) 3.0×10^5 (c) 4.0×10^5.

In order to confirm the repeatability of the results, all cells in the paper were cultured in three Si containers to achieve multiple experiments. And each container with cells and culture medium inside was measured for three times. The preliminary measurement results can be obtained directly by the analysis module (TAS7500, Advantest). Then, statistical analyses were conducted by calculating the values and the standard deviations of the results collected from several measurements.

3. Principles

According to the propagation law of the evanescent wave, the reflection coefficient of prism-wafer interface r_{12} can be expressed by

$$r_{12} = 1 - e^{\pm\kappa d_0} \tag{1}$$

Here, d_0 indicates the thickness of the air layer, and κ is the constant related to the wave vector. Ideally, there is no air layer between Si prism and Si wafer, and r_{12}=0. In this situation, considering that the ATR prism is made of the same material as the Si wafer, all the THz wave energy is transmitted from the upper surface of the Si prism to the upper surface of the Si wafer. The attenuated total reflection occurs on the upper surface of Si wafer, and the THz wave is interacted with the sample in the Si container. The THz penetration depth d_p are illustrated in the following equation

$$d_{\mathrm{p}} = \frac{\lambda}{2\pi n_1\sqrt{\sin^2\theta - \left(\frac{n_2}{n_1}\right)^2}} \tag{2}$$

where λ is the wavelength of THz wave, n_1 is the refractive index of Si wafer (n_1=3.42), n_2 is the refractive index of sample, and θ is the incident angle (θ=57°). The penetration depth d_{p} of the evanescent field (about 24 μm for distilled water at 1 THz) is greater than the thickness of the cell monolayer (around 10 μm). The rest of the THz energy will incident into the cell culture medium. The whole system forms the 'Si-cell-medium' two-interface sample model, as shown in Fig. 3(a).

Then, the cell culture medium in the Si container is sucked away by pipette. The measurement should be done as soon as possible taking water evaporation into account. The process is restricted within 20 seconds to maintain the viability of cells. The penetration depth of the evanescent wave is greater than the thickness of the monolayer cell, and the rest energy of the THz wave will incident into the air. The model can be explained by the 'Si-cell' single-interface sample model, as shown in Fig. 3(b). It can also be understood as the 'Si-cell-air' two-interface sample model.

On the condition of unknown thickness of living cell monolayer d_1, in order to determine the complex refractive index of the cell monolayer only and eliminate the interference of culture medium above the cell monolayer, optical admittance analysis method in film optics is introduced

Biomedical Optics EXPRESS

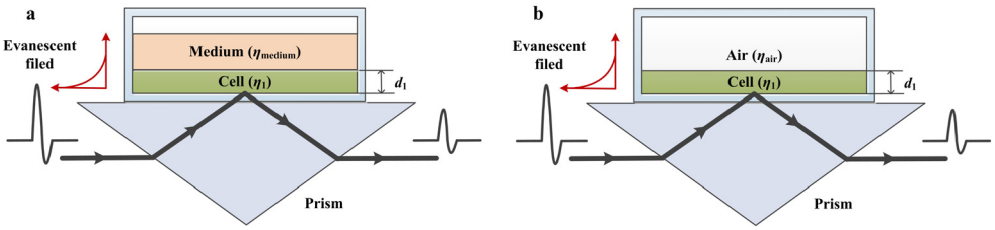

Fig. 3. (a) 'Si-cell-medium' two-interface model; (b) 'Si-cell' single-interface model.

here. The cell monolayer can be regarded as optical films and plated on the surfaces of the cell culture medium and the air medium, respectively. The transfer matrix M of the two-interface medium satisfies the equation as below,

$$M = \begin{bmatrix} \cos\delta_1 & \frac{i}{\eta_1}\sin\delta_1 \\ i\eta_1\sin\delta_1 & \cos\delta_1 \end{bmatrix} \tag{3}$$

Here, M stands for transmission characteristics between the cell monolayer and the medium or air, and η_1 is the optical admittance of the cell monolayer. The phase difference δ_1 is related to the thickness of the living cell monolayer d_1. Thus, the optical admittances of 'Si-cell-medium' and 'Si-cell-air' two-interface models are illustrated as $Y_{\text{cell+medium}}$ and $Y_{\text{cell+air}}$ in Eqs. (4) and (5), respectively.

$$Y_{\text{cell + medium}} = \frac{i\eta_1\sin\delta_1 + \eta_{\text{medium}}\cos\delta_1}{\cos\delta_1 + \frac{i\eta_{\text{medium}}}{\eta_1}\sin\delta_1} \tag{4}$$

$$Y_{\text{cell + air}} = \frac{i\eta_1\sin\delta_1 + \eta_{\text{air}}\cos\delta_1}{\cos\delta_1 + \frac{i\eta_{\text{air}}}{\eta_1}\sin\delta_1} \tag{5}$$

Here, η_{medium} and η_{air} are the optical admittance of culture medium and the air medium, respectively. By solving Eqs. (4) and (5), the optical admittance of cell monolayer η_1 can be obtained by

$$\eta_1 = \sqrt{\frac{\eta_{\text{air}}Y_{\text{cell + air}}(\eta_{\text{medium}} - Y_{\text{cell + medium}}) - \eta_{\text{medium}}Y_{\text{cell + medium}}(\eta_{\text{air}} - Y_{\text{cell + air}})}{(\eta_{\text{medium}} - Y_{\text{cell + medium}}) - (\eta_{\text{air}} - Y_{\text{cell + air}})}} \tag{6}$$

Obviously, the optical admittance of cell monolayer η_1 is independent of cell thickness d_1. Furthermore, the relationship between the optical admittance η_j and the complex refractive index N_j (for P-polarization wave) is given by

$$\eta_j = N_j/\cos\theta = (n + ik)/\cos\theta \tag{7}$$

where n and k stand for the refractive index and the extinction coefficient of sample, respectively. It is clearly seen that, the dielectric responses of living cell monolayer can be obtained by the combination of single-interface and two-interface ATR models. Here, it should be mentioned that, the light spot of THz wave on the surface of the ATR prism was nearly 10 mm in size, which was much larger than the cell size. The impact of inhomogeneity of the cell culture monolayer could be ignored due to the macroscopic measurement for several times.

4. Results and discussion

Firstly, to prove the feasibility of the experiment system in Fig. 1, the THz spectrum of RPMI 1640 culture medium was measured through dripping the RPMI 1640 culture medium on the

Biomedical Optics EXPRESS

bottom of the Si containers. The time domain pulses before and after placing culture medium on the Si container were collected as the reference and the signal, indicated by red and blue solid lines in Fig. 4(a), respectively. The first signal peak at 17ps was caused by the air-layer between the Si wafer and the ATR prism, at which time the THz wave was reflected by the lower surface of the Si wafer. The second signal peak occurred at 31ps while the THz wave was reflected by the upper surface of the Si wafer, where THz wave was interacted with the RPMI 1640 culture medium. Moreover, the time difference between the first and the second time-domain peak stood for the thickness of the Si wafer. To ensure the accuracy of the experiment results, the amplitude and time of the first time-domain peak for the sample measurements should be consistent with those for the background measurements. In other words, the thickness of the air layer should be unchanged during the measurement alternation between reference and sample.

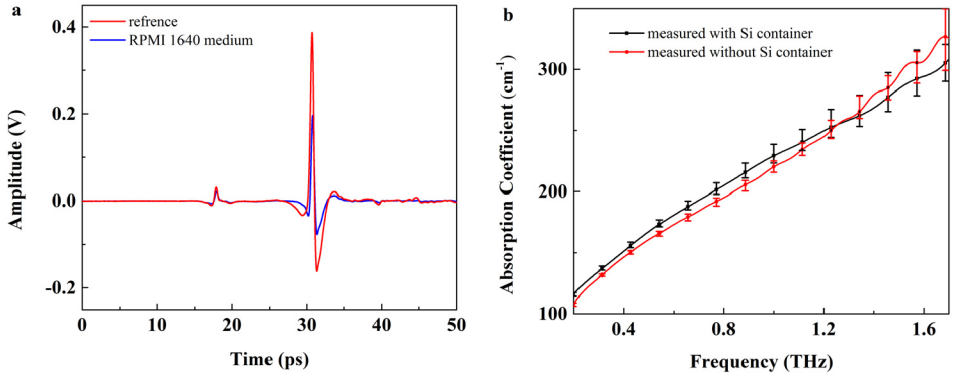

Fig. 4. (a) The time-domain signal of RPMI 1640 culture medium (blue solid line) and reference (red solid line) with Si container. (b) The absorption coefficients of RPMI 1640 cell culture medium measured with Si container (black solid line) and measured without Si container (red solid line).

Figure 4(b) shows the absorption coefficients of RPMI 1640 culture medium were measured using the ATR-TDS system with Si container (black solid line) and without container (red solid line), respectively. The measurements were performed for five times and the average absorption coefficients were obtained. The curves of the two methods were nearly consistent, indicating that ATR-TDS equipped with the Si container was a feasible technique. The slight difference between the two curves came from the pressure caused by the weight of the RPMI 1640 culture medium, which could affect the thickness of air layer. Because the cell sample has relative light weight, the effect of this factor could be ignored. However, the pressure caused by the sample weight as well as the pressure above the sample should be kept stable for the high precise measurements [23]. Especially for the heavy sample measurement, the thickness of air layer would be clearly different from the reference. The additional object should be applied above the Si container to generate the same pressure caused by the sample weight, and it should be altered according to the sample weight. This would make the experimental procedure a little complicated.

Then, the sample composed of the living PC12 cells (the number of cells is 4×10^5) and the RPMI 1640 culture medium were measured by THz-TDS system after attaching Si container onto the prism closely. As shown in Fig. 5, the red solid lines showed the complex refractive index based on the two-interface 'Si-cell-medium' model, i.e., the refractive index and extinction coefficient. Then, the pipette was employed to suck away the RPMI 1640 culture medium. In order to maintain the viability of cells and keep intracellular water unchanged, the spectral measurements must be completed within a certain time. We monitored the same sample of single-interface 'Si-cell' model in 1 min with THz-TDS system. The inset of Fig. 5 shows the

Biomedical Optics EXPRESS

detailed results, where the pink, purple, wine, green solid lines indicated the complex refractive index based on the single-interface 'Si-cell' model in 10seconds, 20seconds, 30seconds and 60seconds, respectively. No significant changes of the complex refractive index of PC12 cells were observed in 30seconds. After 1 min, the refractive index becomes lower, which may be attributable to the water evaporation and the changes in intracellular hydration states. The extinction coefficient decrease slightly within 1 min. Thus, it is reasonable that the effects of cell viability and water evaporation are negligible in case that the operation procedure including the detection time is less than 30seconds. In our experiments, the spectral measurement time is set within 20seconds. Furthermore, the blue dash lines showed the dielectric properties of PC12 cell monolayer solved using Eqs. (6) and (7). Considering the error for the blue dash lines depends on single-interface and two-interface ATR measurements, which is a function of $Y_{cell+DMEM}$ and $Y_{cell+air}$, the error bars don't be displayed in the results. In order to better compare the difference between the red solid lines and the blue dashed lines, the inset was provided in Fig. 5, depicting the details in the range of 0.7–0.8 THz. Obviously, it can be seen that the blue dashed lines deviated from the red solid lines slightly, especially for the extinction coefficient, which were consistent with the previous reports [17,18]. In other words, the dielectric parameters deduced directly through 'Si-cell-medium' model measurement still has some errors due to the information of culture medium included. However, the accurate dielectric properties of living glial-like cell monolayer can be obtained by combination of single-interface and two-interface ATR models. Overall, the refractive index and extinction coefficient decreased with the THz frequency increase. Additionally, after removing the RPMI 1640 culture medium, the cell monolayer was dried by flowing air for 5mins to make the culture medium evaporation completely. The black solid lines showed the complex refractive index of sample composed of dehydrated PC12 cell monolayer and air. The refractive index and extinction coefficient are close to the parameters of air. The significant difference in the absorption came from the change of intracellular fluid, such as hydration water and free water.

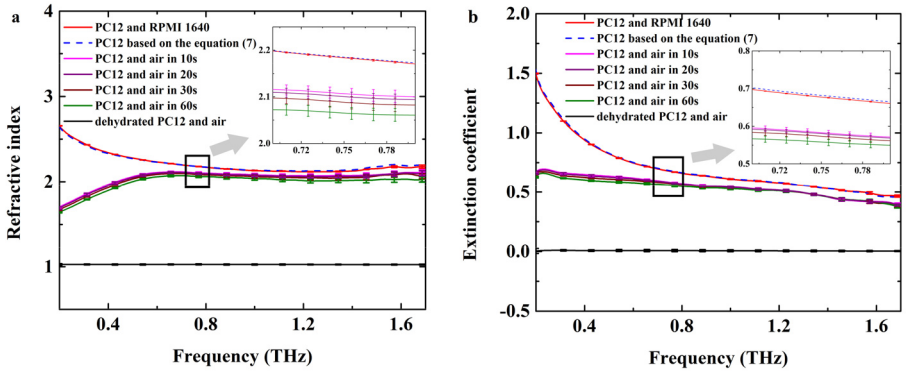

Fig. 5. The complex refractive index of living PC12 cell monolayer from rats. (a) refractive index, (b) extinction coefficient. The red solid lines showed the dielectric properties based on two-interface 'Si-cell-medium' model. The blue dashed lines showed the dielectric properties of PC12 cell monolayer based on Eq. (7). The black solid lines showed the dielectric properties of sample composed of the dehydrated PC12 cell monolayer and the air medium. The pink, purple, wine, green solid lines showed the the complex refractive index based on the single-interface 'Si-cell' model in 10seconds, 20seconds, 30seconds and 60seconds, respectively.

The effect of living cell numbers on dielectric properties has been studied. The living PC12 cells were cultured in the Si containers with the numbers of 2×10^5, 3×10^5 and 4×10^5, respectively. As shown in Fig. 6, the solid lines showed the dielectric properties based on

Biomedical Optics EXPRESS

two-interface 'Si-cell-medium' model. The dashed lines showed the dielectric responses of PC12 cell monolayer solved by Eqs. (6) and (7). The complex refractive index of living PC12 cell monolayer showed a positive relation to the cell number. As the number of living PC12 cells increased, the refractive index was increased and the extinction coefficient was decreased. The changes became apparent with the THz frequency increase. When the number of living PC12 cells was equal to 4×10^5, the absorption was lower than the others. It can be induced that, the content of the culture medium in the intercellular space was relatively decreased with the cell number increasing. Accordingly, the THz absorption will decrease with the cell number increase.

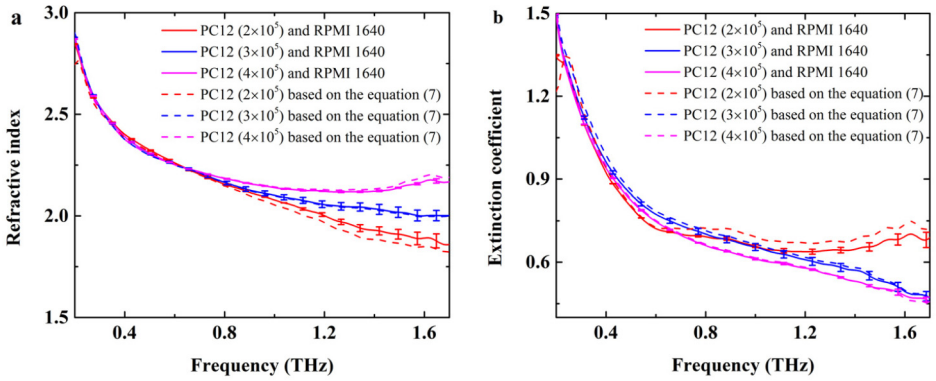

Fig. 6. The complex refractive index for different numbers of living PC12 cells from rats (a) Refractive index, (b) extinction coefficient. The solid lines showed the dielectric properties based on two-interface 'Si-cell-medium' model. The dashed lines showed the dielectric responses of PC12 cell monolayer based on Eq. (7). The red, blue, pink curves were the dielectric responses for the cell number of 2×10^5, 3×10^5 and 4×10^5, respectively.

In order to compare the glioma cells with normal glial-like cells, the C6 glioma cells from rats with the number of 2×10^5 were cultured using DMEM medium. And the dielectric responses of the C6 glioma cells were measured under the same conditions for PC12 cell monolayer mentioned above, such as the same Si container, the same room temperature and dryness of air. The results of spectral measurements were shown in Fig. 7. The dielectric properties of two-interface medium composed of living cell monolayer and culture medium (solid lines) were directly obtained by spectroscopy measurements, while the dielectric properties of cell monolayer (dashed lines) were solved using Eqs. (6) and (7). The curves almost overlapped together. For better comparison, the spectra of PC12 cells were also depicted in Fig. 7. The results showed that C6 glioma cell monolayer (blue dashed lines) and PC12 cell monolayer (red dashed lines) had different spectral characteristics at the cell number of 2×10^5. The refractive index of C6 tumor cell monolayer was higher than that of PC12 cell monolayer, and the difference increases with the THz frequency increase. Considering the culture mediums are different for the two kinds of cells, the ATR spectral measurements for RPMI 1640 medium and DMEM medium were performed for five times, as shown in the insets of Fig. 6. The discrepancy of the dielectric properties is very small. Thus, the difference of refractive indices between C6 tumor cell monolayer and PC12 cell monolayer might mainly originates from different cell structures. The absorption properties of PC12 cell monolayer were nearly the same as those of C6 cell monolayer.

Furthermore, the living glial-like cell monolayers derived from human were investigated. The SVG P12 cell is human astrocyte, and the HMO6 cell is human microglial. SVG P12 cell and HMO6 cell were cultured using DMEM with the cell number of 3×10^5. The process of living cell culture was the same as above. Figure 8 shows the dielectric responses of two-interface model composed of living human cell monolayer and culture medium (solid lines) were clearly

Biomedical Optics EXPRESS

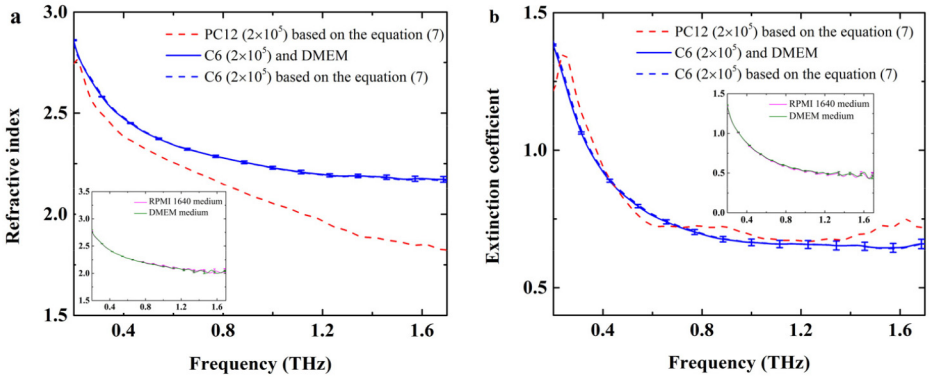

Fig. 7. The complex refractive index for PC12 and C6 cells from rats. (a) Refractive index, (b) extinction coefficient. The blue solid line was the dielectric properties of two-interface medium composed of living C6 cell monolayer and culture medium. The blue dashed line and the red dashed line were the dielectric properties of C6 and PC12 cell monolayers based on Eq. (7), respectively. The insets showed the dielectric properties of RPMI 1640 culture medium and DMEM medium.

different from the dielectric responses of cell monolayer (dashed lines) solved using Eqs. (6) and (7), especially for SVG P12 cell. Moreover, we found that there were significant differences in the refractive index and extinction coefficient between SVG P12 living cell monolayer (red dashed lines) and HMO6 living cell monolayer (blue dashed line) in the range of 0.2–1.2THz. It could be mainly attributed to the cell structure, including the cell size and cell morphology. In addition, the arrangement of different cell types may be different even in the case of cell monolayer. The effect of the layer number and the cell arrangement direction should be discovered in the further study.

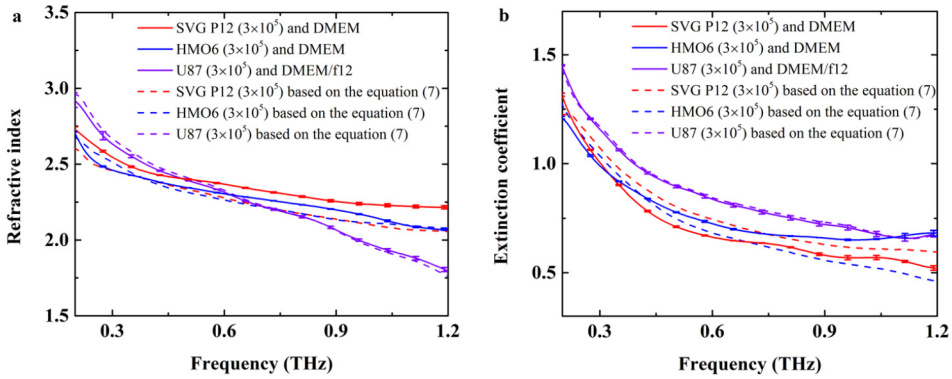

Fig. 8. The complex refractive index for SVG P12 cells, HMO6 cells, and U87 cells. (a) Refractive index, (b) extinction coefficient. The solid lines showed the dielectric responses based on two-interface 'Si-cell-medium' model, the dash lines showed the dielectric responses for human cells based on Eq. (7). The red, blue, purple cures showed the dielectric responses for SVG P12 cells, HMO6 cells and U87 cells, respectively.

For comparison, the human glioma U87 cells were also detected and analyzed. The culture medium of U87 cells was DMEM/f12. Figure 8. showed that the absorption of glioma U87 monolayer (purple dashed lines) was larger than that of SVG P12 cell monolayer and HMO6 cell monolayer. Based on the combination of single-interface and two-interface ATR models, the

Biomedical Optics EXPRESS

significant differences were observed between glioma cells and normal glial-like cells derived from human. This result is in agreement that brain glioma tissue has higher refractive index and absorption coefficient than those of normal tissue [24,25]. In other words, this study illustrated that THz wave can be used for the diagnosis of glioma at the cellular level.

5. Conclusion

The attenuated total reflection spectroscopy with the Si container attached on the ATR prism has been demonstrated to be an efficient method to obtain the dielectric properties of living cells in THz range. According to the optical admittance analysis, the dielectric responses of living cell monolayers can be determined without cell thickness based on the combination of the single-interface and the two-interface models. The characteristics of different kinds of living cells with different cell numbers have been experimentally measured using ATR THz-TDS system. Furthermore, the glioma cells exhibited different dielectric properties compared with the normal cells, which can account for the glioma tissue discrimination using THz wave. This method will provide a new insight to in situ fast monitoring of living cells accurately.

Funding

China Postdoctoral Science Foundation ((2016M602954)); Joint Incubation Project of Southwest Hospital ((SWH2016LHJC-04, SWH2016LHJC-01)); National Basic Research Program of China (973 Program) (2015CB755403); National Natural Science Foundation of China (61771332, 61775160); Chongqing Postdoctoral Science Foundation (Xm2016021).

Disclosures

The authors declare that there are no conflicts of interest related to this article.

References

1. V. P. Wallace, A. J. Fitzgerald, E. Pickwell, R. J. Pye, P. F. Taday, N. Flanagan, and T. Ha, "Terahertz pulsed spectroscopy of human Basal cell carcinoma," Appl. Spectrosc. **60**(10), 1127–1133 (2006).
2. M. K. Kuimova, K. L. Chan, and S. G. Kazarian, "Chemical imaging of live cancer cells in the natural aqueous environment," Appl. Spectrosc. **63**(2), 164–171 (2009).
3. J. Bock, Y. Fukuyo, S. Kang, M. L. Phipps, L. B. Alexandrov, K. Rasmussen, A. R. Bishop, E. D. Rosen, J. S. Martinez, H. T. Chen, G. Rodriguez, B. S. Alexandrov, and A. Usheva, "Mammalian Stem Cells Reprogramming in Response to Terahertz Radiation," PLoS One **5**(12), e15806 (2010).
4. C. B. Reid, G. Reese, A. P. Gibson, and V. P. Wallace, "Terahertz Time-Domain Spectroscopy of Human Blood," IEEE Trans. Terahertz Sci. Technol. **3**(4), 363–367 (2013).
5. S. J. Park, J. T. Hong, S. J. Choi, H. S. Kim, W. K. Park, S. T. Han, J. Y. Park, S. Lee, D. S. Kim, and Y. H. Ahn, "Detection of microorganisms using terahertz metamaterials," Sci. Rep. **4**(1), 4988 (2015).
6. X. Yang, X. Zhao, K. Yang, Y. P. Liu, Y. Liu, W. L. Fu, and Y. Luo, "Biomedical Applications of Terahertz Spectroscopy and Imaging," Trends Biotechnol. **34**(10), 810–824 (2016).
7. L. Shi, P. Shumyatsky, A. Rodríguez-Contreras, and R. Alfano, "Terahertz spectroscopy of brain tissue from a mouse model of Alzheimer's disease," J. Biomed. Opt. **21**(1), 015014 (2016).
8. G. G. Hernandez-Cardoso, S. C. Rojas-Landeros, M. Alfaro-Gomez, A. I. Hernandez-Serrano, I. Salas-Gutierrez, E. Lemus-Bedolla, A. R. Castillo-Guzman, H. L. Lopez-Lemus, and E. Castro-Camus, "Terahertz imaging for early screening of diabetic foot syndrome: A proof of concept," Sci. Rep. **7**(1), 42124 (2017).
9. C. M. Hough, D. N. Purschke, C. Huang, L. V. Titova, O. Kovalchuk, and B. J. Warkentin, "Biological effects of intense THz pulses on human skin tissue models," *IRMMW-THz*, 1–3 (2017).
10. J. S. Olshevskaya, A. S. Ratushnyak, A. K. Petrov, A. K. Kozlov, and T. A. Zapara, "Effect of terahertz electromagnetic waves on neurons systems," In *Computational Technologies in Electrical and Electronics Engineering, 2008. SIBIRCON 2008. IEEE Region 8 International Conference on*. IEEE, 210–211 (2008).
11. M. V. Duka, L. N. Dvoretskaya, N. S. Babelkin, M. K. Khodzitskii, S. A. Chivilikhin, and O. A. Smolyanskaya, "Numerical and experimental studies of mechanisms underlying the effect of pulsed broadband terahertz radiation on nerve cells," Quantum Electron. **44**(8), 707–712 (2014).
12. J. B. Masson, M. P. Sauviat, J. L. Martin, and G. Gallot, "Ionic contrast terahertz near-field imaging of axonal water fluxes," Proc. Natl. Acad. Sci. U. S. A. **103**(13), 4808–4812 (2006).

Biomedical Optics EXPRESS

13. A. Araque and M. Navarrete, "Glial cells in neuronal network function," Philos. Trans. R. Soc., B **365**(1551), 2375–2381 (2010).
14. M. Hanani, "Satellite glial cells in sensory ganglia: from form to function," Brain Res. Rev. **48**(3), 457–476 (2005).
15. M. Borovkova, M. Serebriakova, V. Fedorov, E. Sedykh, V. Vaks, A. Lichutin, A. Salnikova, and M. Khodzitsky, "Investigation of terahertz radiation influence on rat glial cells," Biomed. Opt. Express **8**(1), 273 (2017).
16. P. Weightman, "Prospects for the study of biological systems with high power sources of terahertz radiation," Phys. Biol. **9**(5), 053001 (2012).
17. H. B. Liu, G. Plopper, S. Earley, Y. Chen, B. Ferguson, and X. C. Zhang, "Sensing minute changes in biological cell monolayers with THz differential time-domain spectroscopy," Biosens. Bioelectron. **22**(6), 1075–1080 (2007).
18. K. Shiraga, Y. Ogawa, T. Suzuki, N. Kondo, A. Irisawa, and M. Imamura, "Determination of the complex dielectric constant of an epithelial cell monolayer in the terahertz region," Appl. Phys. Lett. **102**(5), 053702 (2013).
19. K. Shiraga, Y. Ogawa, T. Suzuki, N. Kondo, A. Irisawa, and M. Imamura, "Characterization of dielectric responses of human cancer cells in the terahertz region," J. Infrared, Millimeter, Terahertz Waves **35**(5), 493–502 (2014).
20. M. Grognot and G. Gallot, "Quantitative measurement of permeabilization of living cells by terahertz attenuated total reflection," Appl. Phys. Lett. **107**(10), 103702 (2015).
21. K. Shiraga, T. Suzuki, N. Kondo, K. Tanaka, and Y. Ogawa, "Hydration state inside HeLa cell monolayer investigated with terahertz spectroscopy," Appl. Phys. Lett. **106**(25), 253701 (2015).
22. Y. Zou, Q. Liu, X. Yang, H. C. Huang, J. Li, L. H. Du, Z. R. Li, J. H. Zhao, and L. G. Zhu, "Label-free monitoring of cell death induced by oxidative stress in living human cells using terahertz ATR spectroscopy," Biomed. Opt. Express **9**(1), 14–24 (2018).
23. J. Wang, R. I. Stantchev, S. Sun, T. W. Chiu, A. T. Ahuja, and E. Pickwell-MacPherson, "THz in vivo measurements: the effects of pressure on skin reflectivity," Biomed. Opt. Express **9**(12), 6467–6476 (2018).
24. Y. Peng, W. Chen, and Y. Zhu, "Identification of Biomarker (L-2HG) in Real Human Brain Glioma by Terahertz Spectroscopy," *CLEO: Applications and Technology*, (2018).
25. Z. R. Li, K. Meng, T. N. Chen, T. Chen, L. G. Zhu, Q. Liu, Z. Li, and F. Li, "Identify paraffin-embedded brain glioma using terahertz pulsed spectroscopy," Proc. SPIE **9444**, 94440P (2015).